IEEE Access
Multidisciplinary | Rapid Review | Open Access Journal

Received November 28, 2017, accepted January 4, 2018, date of publication January 9, 2018, date of current version March 16, 2018.

Digital Object Identifier 10.1109/ACCESS.2018.2791417

Dual-Band Circularly Polarized Aperture Coupled Rectangular Dielectric Resonator Antenna for Wireless Applications

ANSHUL GUPTA[1,2] AND RAVI KUMAR GANGWAR[2], (Member, IEEE)
[1]Department of Electronics and Telecommunication Engineering, National Institute of Technology at Raipur, Raipur 492010, India
[2]Department of Electronics Engineering, IIT (Indian School of Mines), Dhanbad 826004, India

Corresponding author: Anshul Gupta (agupta.etc@nitrr.ac.in)

ABSTRACT This paper examines a dual-band circularly polarized (CP) Rectangular Dielectric Resonator Antenna (RDRA). The RDRA is excited by using triangular ring-shaped aperture and an additional parasitic strip, which is connected to the one side of the RDRA. Three striking features of the proposed design are: (i) modified feeding structure (triangular ring-shaped aperture along with microstrip line) and parasitic strip create dual-radiating modes in the RDRA (i.e. $TE^{y}_{1,\delta,1}$ and $TE^{y}_{1,4,1}$); (ii) modified feeding structure with parasitic strip generates CP wave in both the frequency bands; and (iii) The left-hand circular polarization (LHCP) and right-hand circular polarization (RHCP) of proposed antenna can be controlled by taking the mirror image of triangular ring-shaped aperture and parasitic strip. Simulated outcomes have been practically confirmed with the help of developed prototype of the proposed antenna. Measured and simulated results show high harmony to each other. The experimental results confirm that the proposed RDRA is operated over two frequency bands, i.e., 3.4–3.58 GHz and 5.1–5.9 GHz. The 3-dB axial ratio bandwidth of the proposed antenna is about 3.46–3.54 GHz (LHCP) and 5.18–5.34 GHz (RHCP) in lower and upper frequency band, respectively. The proposed antenna is fairly applicable for worldwide interoperability for microwave access and wireless local area network applications.

INDEX TERMS Circular polarization, dielectric resonator antenna, dual band, aperture coupling, WiMAX, WLAN.

I. INTRODUCTION

The Dielectric Resonator Antenna (DRA) is the emerging candidate for various wireless applications because it can be utilized as the substitute to conventional metallic antennas. The DRAs are superior in terms of smaller size, higher radiation efficiency, flexibility in excitation techniques, and achieving variety of radiation characteristics with the help of different mode patterns [1], [2]. The resonant frequency of any DRA mainly depends on the size, shape and dielectric constant of the dielectric material used as the Dielectric Resonator (DR). According to shapes, the rectangular-shaped DRA is advantageous over cylindrical- and hemispherical-shaped DRAs due to the flexibility in selecting the appropriate aspect ratio. Therefore, the antenna engineers are very comfortable to use rectangular DRs. Also, it is easy to achieve the anticipated profile and impedance bandwidth characteristics for rectangular DRs. The DRAs are also better in terms of higher radiation efficiency due to absence of surface wave and wider bandwidth as compared to microstrip antenna [3].

In recent times, the demand of antennas providing dual-band/multiband and wideband characteristics has increased. An antenna having single DR can provide applications in distinct frequency bands. In case of antennas providing wideband, the unwanted frequency spectrum (noise) may degrade the quality of desired frequency spectrum. Such difficulties of unwanted noise can be overcome by dual-/multi-band antennas [4]. Meanwhile, the compact communication devices useful for dual/multiple applications are demanding. So, the antenna designer gained interest in the design of single antenna which can provide multiple frequency bands as well as stable radiation properties over the respective bands. In open literature, several methods are reported for multi-band antennas including use of hybrid antenna which is a combination of DRA with other resonating antennas [5]–[7], use of parasitic elements along with main resonating

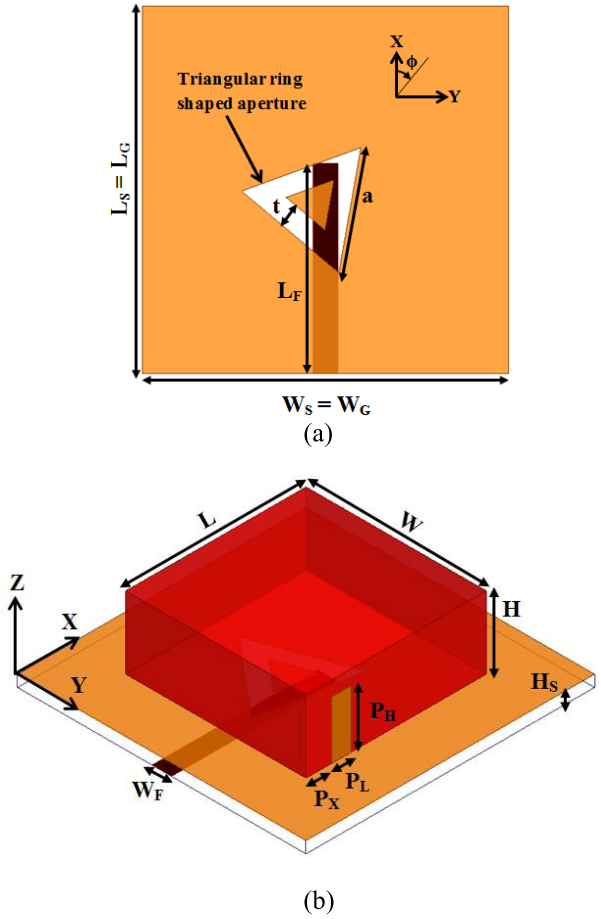

FIGURE 1. Graphical representation of RDRA excited with proposed feed (a) top view (b) 3D view.

structure [8], [9] and use of higher order mode generation [10].

The modern era of mobile communication widely prefer dual-/multi-band circularly polarized antennas in place of linearly polarized antennas due to the advantage of achieving stable link between transmitter and receiver regardless of their orientation. Also, the circularly polarized antennas can minimize the multipath fading efficiency [4]. It is not easy to obtain a dual-band CP DRA using a single DR element as very limited work has been done in the literatures. Some investigations have been reported in the area of single fed dual/circularly polarized DRAs [11]–[15]. Pan *et al.* presented dual-band circularly polarized dielectric resonator antenna (CDRA) with modified circular patch on the top. The CDRA is excited with center probe where drilling is required in substrate and DRA both. Since DRAs are made up of ceramics materials which are very hard so cutting and drilling is always a complex job [11]. Ngan *et al.* proposed singly-fed dual-band CP DRA where two corners of DRA are truncated at 45°. This method reduces the feed complexity but enhances the fabrication complexity and the cost [12]. Similarly Fang and his team mates also designed the dual-band CP DRA where DRA is not only truncated

TABLE 1. Optimized dimensions of various parameters.

S. No.	Parameters	Dimensions
1.	substrate (L_S x W_S x H_S)	40mm x 40mm x 1.6mm
2.	ground plane (L_G x W_G x H_G)	40mm x 40mm x 0.035mm
3.	dielectric resonator antenna (L x W x H)	28mm x 28mm x 8mm
4.	microstrip feed line (L_F x W_F)	22.9mm x 2.7mm
5.	parasitic strip (P_H x P_L)	8mm x 2.7mm
6.	side of triangular aperture (a)	13.86 mm
7.	thickness of triangular aperture (t)	2.6 mm
8.	rotation of triangular aperture (ϕ)	40^0

from two corners but on the top also to tune the ARBW [13]. Lung *et al.* proposed a dual-fed cylindrical DRA where the fundamental HEM_{111} mode and the higher-order HEM_{113} mode are excited to obtain wide AR bandwidths of 12.4% and 7.4% for the lower and upper bands, respectively. Nevertheless, it needs a dual-band quadrature coupler which substantially increases the system size and complexity [14]. Zhang *et al.* [15] proposed the single-fed dual-band CP DRA with 3-dB ARBW of 19.8% and 6.2% for the lower and upper bands respectively. It is found that the lower band is composed of the TE_{111} and TE_{121} modes. TE_{121} is a non-radiating mode and should not be combined with any other radiating mode for bandwidth enhancement purpose which is clearly mentioned in [16]. From the above mention literature review, it can be concluded that dual-band DRAs with lesser fabrication complexity, compact size, and easy tuning of 3-dB ARBW are required. So generation of dual-band CP with suppression of non-radiating mode is also a novelty in the present manuscript.

This article presents a dual-band circularly polarized rectangular dielectric resonator antenna along with triangular ring-shaped aperture and an additional parasitic strip. The analysis of various antenna configurations required for developing the proposed antenna is also included in this article. Some important features of proposed design are: (i) modified feeding structure (triangular ring-shaped aperture along with microstrip line) and parasitic strip create dual radiating modes in the RDRA (i.e. $TE^{y}_{1,\delta,1}$ and $TE^{y}_{1,4,1}$) (ii) modified feeding structure and parasitic strip generate CP wave in both the frequency bands and (iii) The LHCP in first band is achieved due to generation of nearly degenerated modes ($TE^{y}_{1,\delta,1}$ and $TE^{x}_{\delta,1,1}$) with 3-dB ARBW of 3.46-3.54 GHz while the RHCP is generated in second band due to rotated triangular ring-shaped aperture with 3-dB axial ARBW of 5.18-5.34 GHz. (iv) LHCP and RHCP of proposed CDRA can be transformed by taking mirror image of triangular ring-shaped aperture and parasitic strip. The experimental

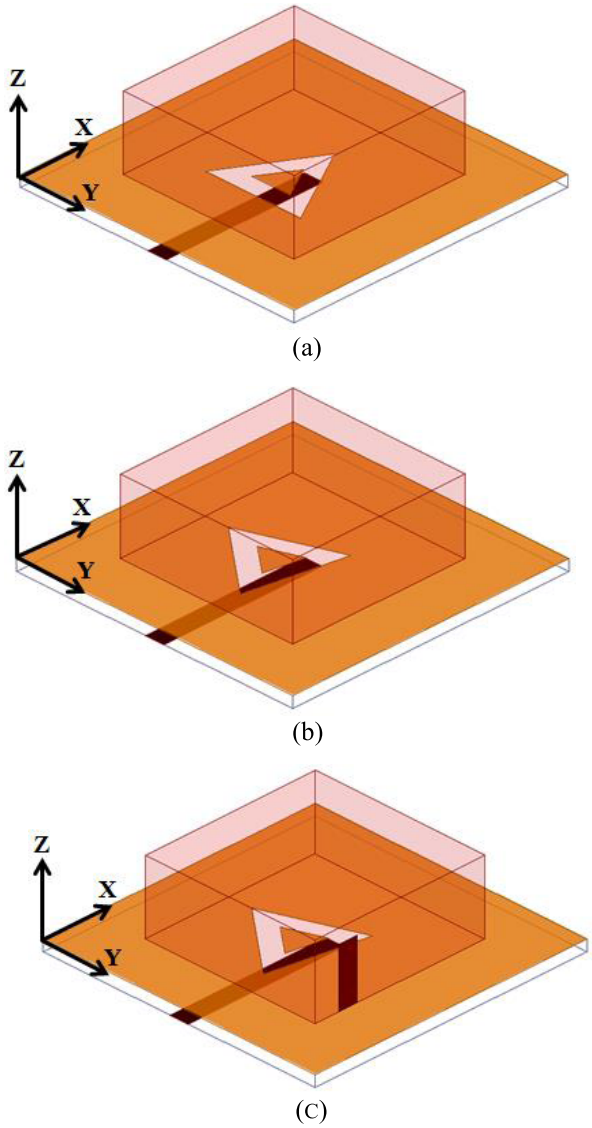

FIGURE 2. Various RDRA antenna configurations (a) antenna-1 (b) antenna-2 (c) antenna-3 (proposed antenna).

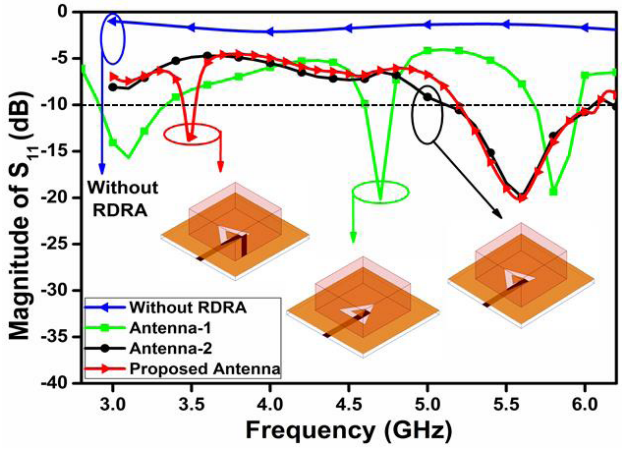

FIGURE 3. Variation of $|S_{11}|$ characteristic of different RDRA antenna configurations.

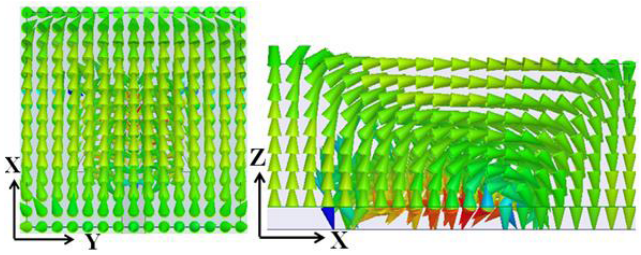

FIGURE 4. Electric field distribution of $TE^{y}_{1,\delta,1}$ mode (a) top view (b) side view.

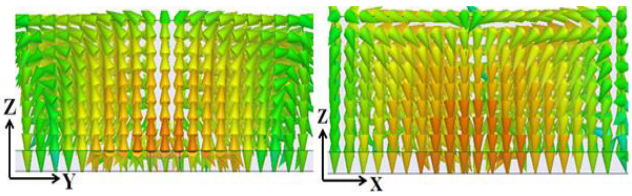

FIGURE 5. Electric field distribution of $TE^{y}_{1,2,1}$ mode (a) front view (b) side view.

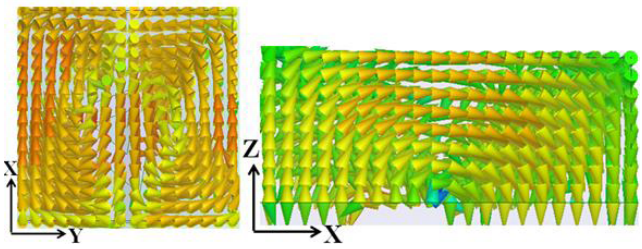

FIGURE 6. Electric field distribution of $TE^{y}_{1,4,1}$ mode (a) top view (b) side view.

results confirm that the proposed RDRA is operated over two frequency bands, i.e., 3.4 GHz-3.58 GHz, and 5.1 GHz – 5.9 GHz. Measured results are in good agreement with the simulated results. The geometry of antenna is presented in Section II. Analysis of proposed structure is described in Section III. Section IV and Section V deal with experimental results and conclusion respectively.

II. ANTENNA GEOMETRY

The triangular ring-shaped aperture and an isometric view of the proposed antenna is shown in the Figure 1(a) and Figure 1(b) respectively. The DRA is made of Alumina ($\varepsilon_r = 9.8, \tan\delta = 0.002$). The triangular ring-shaped aperture is imprinted on the top of the FR4 (Flame Retardant) epoxy substrate ($\varepsilon_r = 4.4, \tan\delta = 0.02$) while the bottom side consists of simple microstrip line i.e. feed line. The thickness of substrate is 1.6 mm. The RDRA is fixed over FR4 substrate with the help of an adhesive (Bonfix). The parasitic strip is cut from an adhesive conducting tap and positioned on the one side of the RDRA. The DRA is designed by using dielectric waveguide model where the transcendental

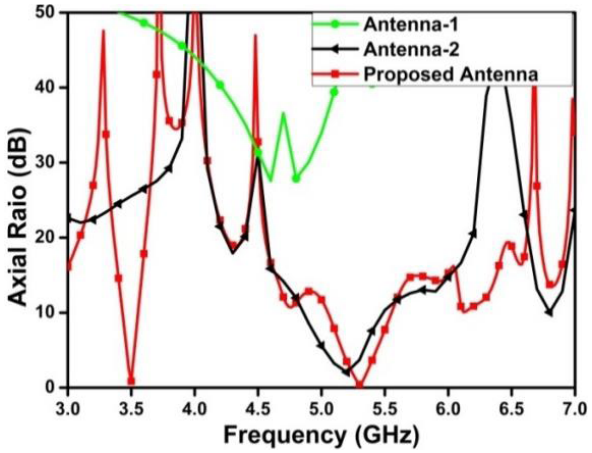

FIGURE 7. Axial ratio variations of different RDRA antenna configurations.

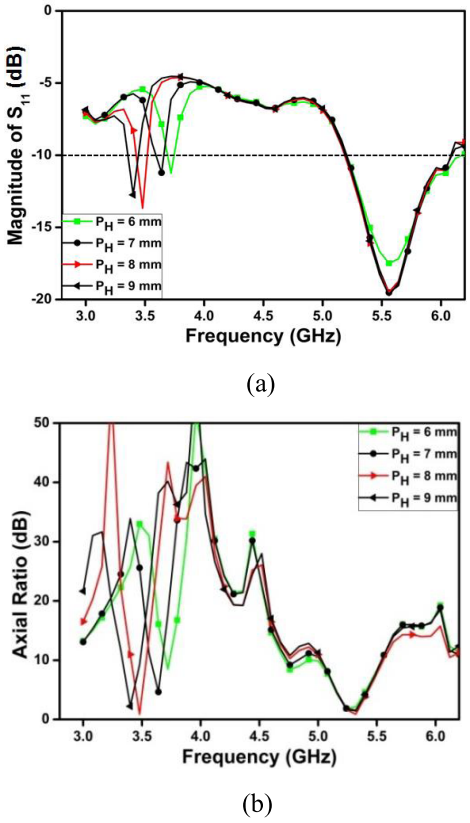

FIGURE 8. Variation of (a) $|S_{11}|$ characteristics and (b) axial ratio for different heights of parasitic strip.

equation has been solved with the help of well-known graphical method [17]. Table 1 contains the dimensions of different optimized parameters.

III. ANTENNA ANALYSIS

This section is concentrated on understanding the phenomenon of generation of dual frequency bands, E-field distribution of higher order modes, LHCP and RHCP operations in proposed antenna. The simulation studies of

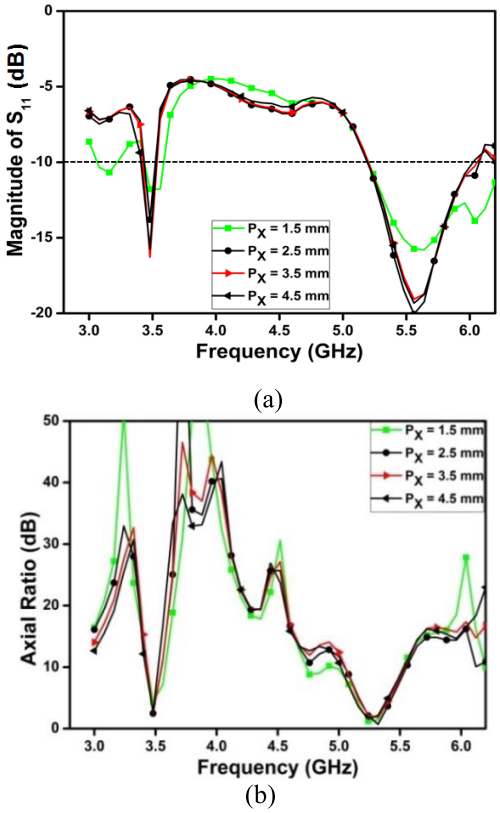

FIGURE 9. Variation of (a) $|S_{11}|$ characteristic and (b) axial ratio for different positions of parasitic strip.

proposed antenna have been carried out using ANSYS High Frequency Structure Simulator (HFSS). This section is again divided into two parts. First part deals with microstrip feed and triangular ring-shaped aperture while the second part is completely concentrated on the parameter variations and observations of parasitic strip.

A. EVOLUTION OF THE PROPOSED ANTENNA STRUCTURE

Figure 2 displays the various RDRA configurations which represent the various steps in developing the proposed antenna for dual band circularly polarized operation. Antenna-1 is the triangular ring-shaped aperture loaded RDRA while in antenna-2, triangular ring-shaped aperture is rotated by 40° with respect to x-axis (as shown in Figure 1). Similarly, a parasitic strip is connected on the one side of RDRA in antenna-3 which is the proposed antenna.

The variation of $|S_{11}|$ characteristics for different resonating RDRA configurations is shown in Figure 3. The very first observation from Figure 3 is that all modes are excited due to the RDRA only. Antenna-1 creates three resonating modes i.e.$TE^{y}_{1,\delta,1}$, $TE^{y}_{1,2,1}$ and $TE^{y}_{1,4,1}$ at resonant frequencies of 3.1 GHz, 4.7 GHz and 5.8 GHz respectively. The E-field distribution of $TE^{y}_{1,\delta,1}$, $TE^{y}_{1,2,1}$ and $TE^{y}_{1,4,1}$ modes are displayed in Figures 4, 5 and 6 respectively. It is depicted that out of three modes, $TE^{y}_{1,\delta,1}$ and $TE^{y}_{1,4,1}$ modes radiate in the broadside direction, while the $TE^{y}_{1,2,1}$ mode has a null in

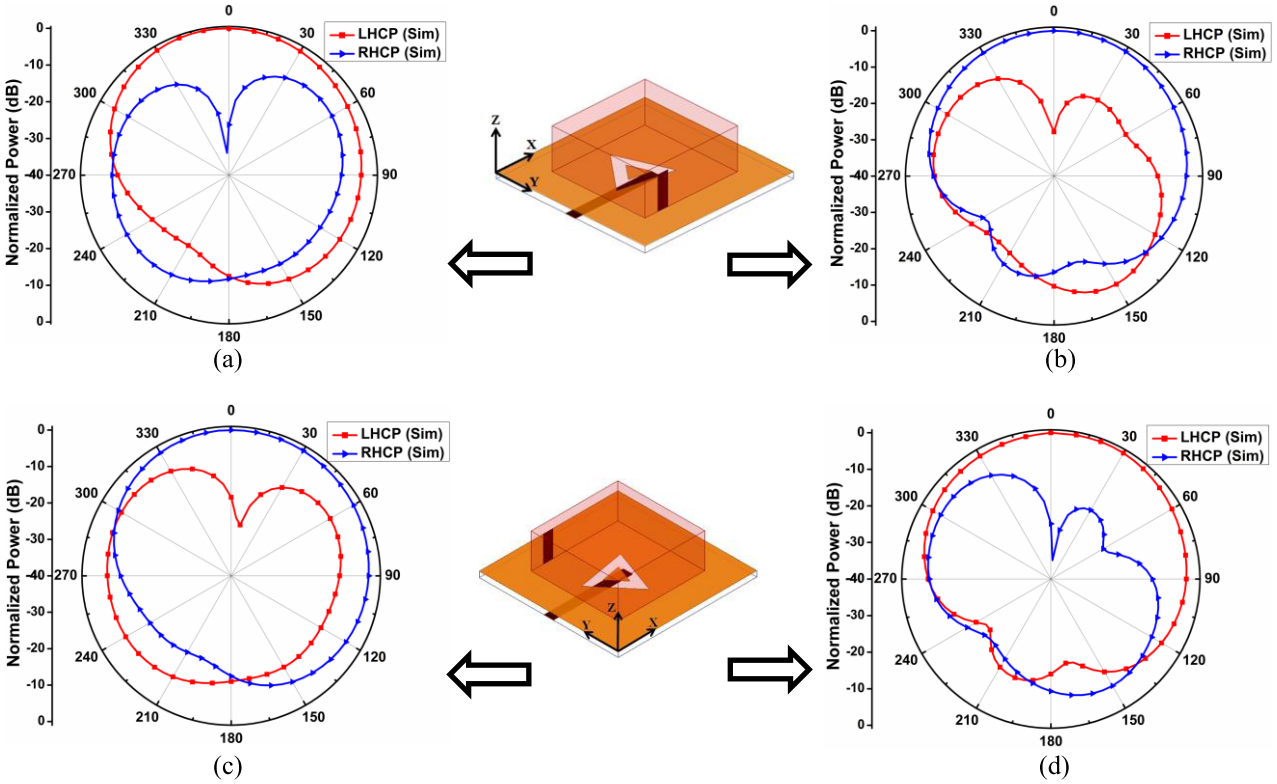

FIGURE 10. Simulated LHCP/RHCP patterns of (a) proposed antenna at 3.5 GHz (b) proposed antenna at 5.26 GHz (c) mirror image of proposed antenna at 3.5 GHz (d) mirror image of proposed antenna at 5.26 GHz.

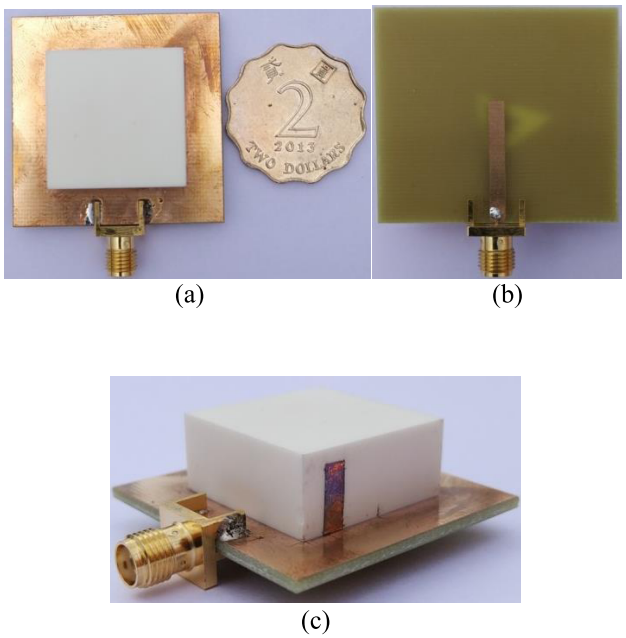

FIGURE 11. Developed prototype of proposed antenna (a) Top view (b) Back view (c) 3D view.

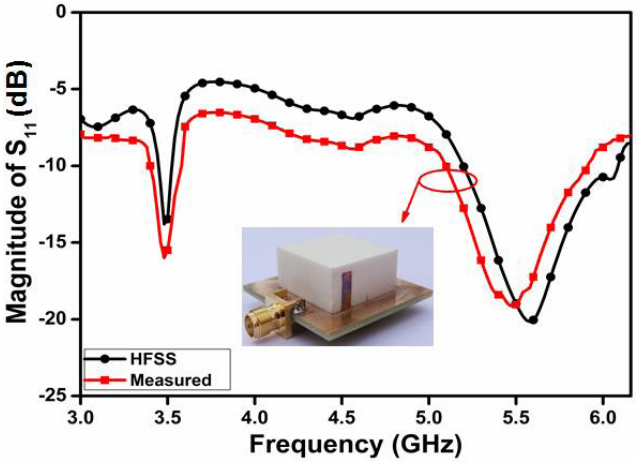

FIGURE 12. Comparison of simulated and measured $|S_{11}|$ characteristic of proposed antenna.

the broadside direction. In antenna-2, triangular ring-shaped aperture has been shifted by 40° which suppress the $TE^{y}_{1,2,1}$ mode and also creates the CP wave in second frequency band (5.2-6.09 GHz) which will be clarified in Figure 7. The reason behind suppression of $TE^{y}_{1,2,1}$ mode is that with the rotation in aperture, $TE^{y}_{1,\delta,1}$ and $TE^{y}_{1,4,1}$ modes satisfied the boundary condition at $z = 0$, the interface between ground plane and resonator, and $z = h$, the interface between air and resonator. However, electric fields of $TE^{y}_{1,2,1}$ mode could not satisfy these particular boundary conditions. Therefore the $TE^{y}_{1,\delta,1}$ mode and $TE^{y}_{1,4,1}$ mode which have the similar radiation

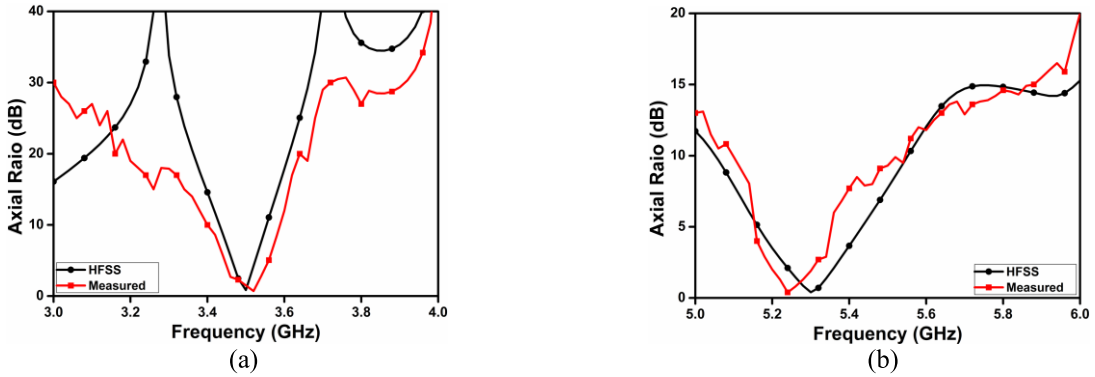

FIGURE 13. Measured and simulated axial ratio ($\theta = 0°; \phi = 0°$) variations of proposed antenna (a) Lower frequency band (b) Upper frequency band.

are excited in this case. $TE^{y}_{1,2,1}$ mode should be suppressed since $TE^{y}_{1,2,1}$ mode is a non-radiating mode and its radiation pattern is equivalent to two opposite magnetic dipoles with approximately the same values [16]. Finally, a parasitic strip is connected to the one side of DRA in antenna-3 which creates the CP wave in first band (3.44-3.53 GHz). Figure 7 displays the axial ratio variations of different RDRA antenna configurations. No CP wave is generated in case of antenna-1. It is known that there are two necessary and sufficient conditions required for creating CP wave in any antenna structure: (i) generation of de-generated orthogonal modes inside the radiating structure; (ii) phase shift between these modes must be 90°. A CP radiation is achieved in first band (at 3.5 GHz) from pair of nearly degenerated modes ($TE^{y}_{1,\delta,1}$ and $TE^{x}_{\delta,1,1}$) in RDRA with axial ratio bandwidth of 3.48-3.52 GHz [18], [19]. $TE^{x}_{\delta,1,1}$ mode is observed in RDRA due to loading of parasitic patch [20]. 90° phase shift between x- and y- polarized E-field lines is generated by 40° rotated triangular ring shaped aperture is accountable for CP wave generation in the second frequency band (5.21-5.39 GHz).

B. PARASITIC STRIP OPTIMIZATION

The variation of $|S_{11}|$ characteristic and axial ratio with the change in height of parasitic strip is shown in Figure 8 (a) and Figure 8 (b) respectively. It's concluded from Figure 8 (a) that as the height of parasitic patch is increased, the resonant frequency of first band shifts towards the lower side while no variation is observed in the second band. This is due to the fact that Parasitic strip changes the electrical length of RDRA in y-direction. Similarly, from Figure 8(b), axial ratio variation is observed in the first frequency band only. This is due to the fact that parasitic strip loaded DR mode (i.e. $TE^{x}_{\delta,1,1}$) is generated in first band only. The variation of $|S_{11}|$ characteristic and axial ratio with the change in the position (P_X, as shown in Figure 1) of parasitic strip is shown in Figure 9 (a) and (b) respectively. It can be concluded from Figure 9 (a) that the position of parasitic strip doesn't make any appreciable change in $|S_{11}|$ characteristics for both the bands. Similarly, it is depicted from Figure 9 (b) that the position of parasitic strip doesn't affect the axial ratio characteristics for both the bands. Thus, the proposed antenna provides the dual-band dual-CP characteristics with the easy tuning of impedance bandwidth and axial ratio.

C. SENSE OF POLARIZATION

Simulated RHCP/LHCP patterns in both the frequency bands for proposed antenna and mirror image of proposed antenna are shown in Figure 10. It is clearly witnessed from Figure 10 that sense of circular polarization has been transformed by taking the mirror image of triangular ring-shaped aperture and parasitic strip. We know that parasitic strip and triangular ring-shaped aperture are the root cause of CP wave in first and second band of CDRA respectively (from aforementioned discussion). As we take the mirror image of parasitic strip and triangular-shaped aperture, clockwise circulation (LHCP) of electric field converted into anticlockwise circulation (RHCP) in first band while the anticlockwise circulation (RHCP) of electric field converted into clockwise circulation (LHCP) in second band.

IV. EXPERIMENTAL RESULTS

To validate the optimized simulated results, the prototype of proposed antenna is developed as shown in Figure 11. Agilent ENA series vector network analyzer with Model No., E5071C (300 kHz-20 GHz) is used to extract the $|S_{11}|$ characteristic of the proposed antenna. Comparison between measured and simulated $|S_{11}|$ characteristic of the proposed antenna is presented in Figure 12. Comparison between simulated and experimental results is shown in Table 2. From Figure 12 and Table 2, it can be determined that the proposed antenna structure cover two different frequency bands, i.e. 3.4 GHz – 3.58 GHz and 5.1 GHz – 5.9 GHz. with a fractional bandwidth of 5.16 % and 14.55 % respectively. The fractional bandwidths are calculated with respect to the center frequency. The measured results are in good agreement with the simulated results. However, some differences between simulated and measured results may be due to effect of an adhesive and SMA (SubMiniature version A, 50Ω) connector.

TABLE 2. Comparison between simulated and measured results.

	Lower Band				Upper Band			
	Impedance Bandwidth (GHz)	Impedance Bandwidth (%)	3-dB ARBW	3-dB ARBW (%)	Impedance Bandwidth (GHz)	Impedance Bandwidth (%)	3-dB ARBW	3-dB ARBW (%)
HFSS	3.44-3.53	2.58	3.48-3.52	1.03	5.2-6.09	15.78	5.21-5.39	3.4
Measured	3.4-3.58	5.16	3.46-3.54	2.29	5.1-5.9	14.55	5.18-5.34	3.04

TABLE 3. Comparison of proposed antenna with other published dual band literature.

		Lower Band		Upper Band	
DRA Shape	Type of Excitation	Operating frequency range (GHz)	Impedance Bandwidth (%)	Operating frequency range (GHz)	Impedance Bandwidth (%)
Rectangular [7]	Aperture coupling	2.4-2.51	4.48	5.03-5.35	6.17
Cylindrical [8]	CPW Feed	3.3-3.61	8.97	4.6-4.91	4.8
Cylindrical [9]	Microstrip line	2.36-2.5	3.3	5.4-5.8	5.7
Proposed RDRA	Triangular aperture	3.4-3.58	5.16	5.18-5.34	14.55

The comparison of proposed antenna with other published dual-band DRA designs on the basis of impedance bandwidth is shown in Table 3. It can be concluded from Table 3 that the proposed RDRA has better impedance bandwidth compared to other exiting dual-band DRA structures.

The proposed antenna has an extra advantage of dual band circular polarization. Figures 13 (a) and (b) show the simulated and measured axial ratio variations of proposed antenna towards broadside direction ($\theta = 0^0$; $\phi = 0^0$) in lower and upper frequency bands respectively. Dual-linear pattern method [21] is used to measure the axial ratio of proposed antenna. It is concluded from Figure 13 that 3-dB ARBW (measured) of proposed antenna in lower and upper frequency band is about 2.29 % (3.46-3.54 GHz) and 3.04 % (5.18-5.34 GHz) respectively.

Figure 14 shows measured and simulated LHCP and RHCP patterns at 3.5 GHz and 5.26 GHz respectively. From Figure 14 (a), it is observed that LHCP patterns are approximately 20 dB greater than RHCP patterns towards broadside direction. This confirms the proposed antenna supports clockwise rotation of CP wave in the first band. Similarly, it is concluded from Figure 14 (b), that RHCP patterns are approximately 20 dB greater than LHCP patterns towards broadside direction. This confirms the proposed antenna supports anti-clockwise rotation of CP wave in the second band. LHCP/RHCP patterns are measured in the anechoic chamber with the help of far-field patterns in elevation (E_E) and azimuthal plane (E_A) [22]. Figure 15 shows measured and simulated gain of proposed antenna (($\theta = 0^0$; $\phi = 0^0$). The value of gain is measured only in shadowed region of Figure 15. There is minor difference between measured and simulated gain value which occurs due to the cable and connector losses occur in the measurement (not considered

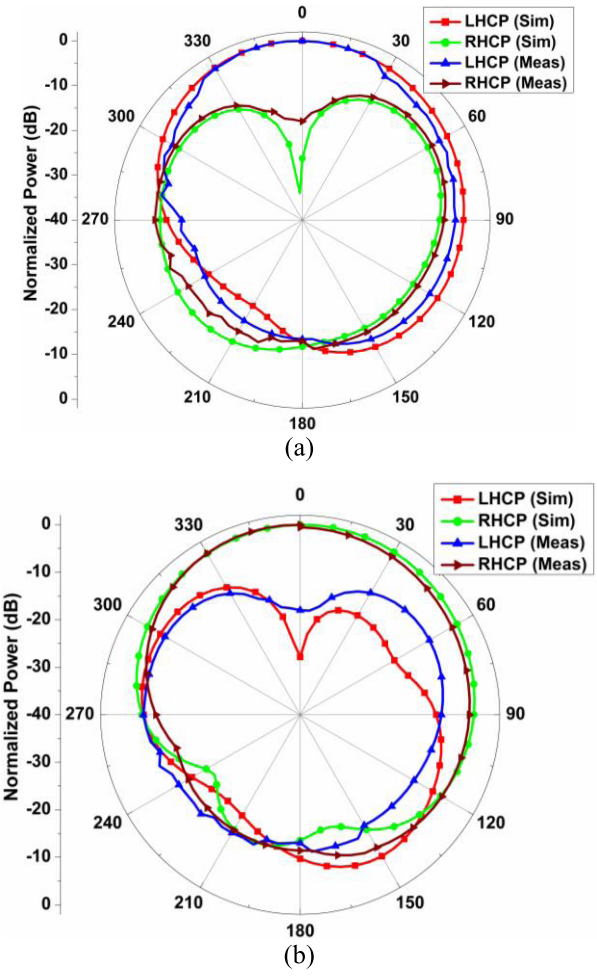

FIGURE 14. Measured and simulated radiation patterns of proposed antenna at (a) 3.5 GHz (LHCP) (b) 5.26 GHz (RHCP).

during simulation). The gain of the proposed antenna is measured with the help of Friss Transmission Formula [4].

$$E_{RHCP} = 0.707(E_A + jE_E) \quad (1)$$

$$E_{LHCP} = 0.707(E_A - jE_E) \quad (2)$$

Figure 16 shows simulated radiation efficiency and directivity versus frequency characteristics of proposed antenna. The simulated radiation efficiencies are 93.73 %, and 96.24 % at resonant frequencies of 3.5 GHz, and 5.26 GHz respectively which evidences that proposed antenna is an efficient radiator.

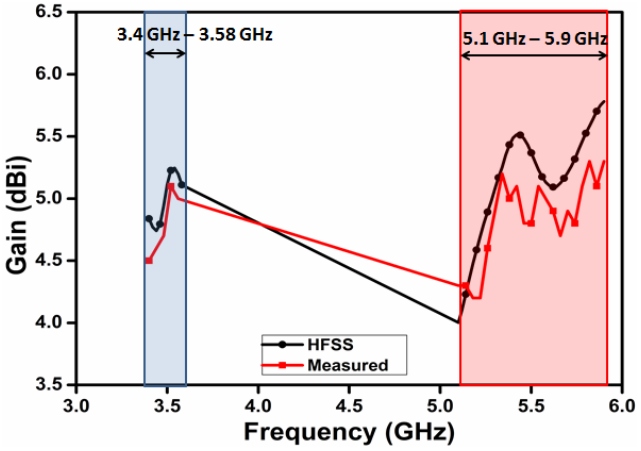

FIGURE 15. Measured and simulated gain variation of proposed antenna ($\theta = 0°; \phi = 0°$).

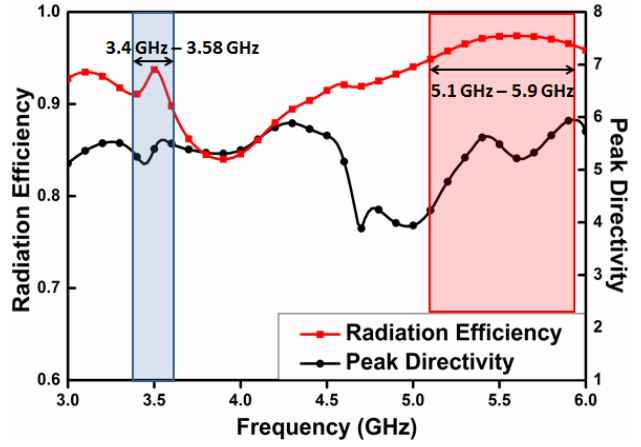

FIGURE 16. Simulated Radiation efficiency and peak directivity variation of proposed antenna.

V. CONCLUSION

This article investigates dual-band circularly polarized rectangular dielectric resonator antenna. The proposed antenna provides two frequency bands i.e., 3.4 GHz – 3.58 GHz, and 5.1 GHz – 5.9 GHz. Another important feature of the proposed antenna is dual-band CP wave i.e. 3.46-3.54 GHz (LHCP) and 5.18-5.34 GHz (RHCP). The CP wave in first band is achieved due to generation of nearly degenerated modes ($TE^{y}_{1,\delta,1}$ and $TE^{x}_{\delta,1,1}$) while 40° rotated triangular ring-shaped aperture is responsible for the CP wave generation in the second band. The proposed feeding structure (microstrip line with triangular ring-shaped aperture) and parasitic strip creates dual radiating modes in the RDRA (i.e. $TE^{y}_{1,\delta,1}$ and $TE^{y}_{1,4,1}$) which radiate in the broadside direction. The impedance bandwidth and axial ratio can be simply controlled with the help of parasitic strip. LHCP/RHCP in both the frequency bands can be altered by taking mirror image of triangular ring-shaped aperture and parasitic strip. These captivating features of the proposed antenna make it appropriate for WiMAX and WLAN applications.

REFERENCES

[1] A. Petosa, A. Ittipiboon, Y. M. M. Antar, D. Roscoe, and M. Cuhaci, "Recent advances in dielectric-resonator antenna technology," *IEEE Antennas Propag. Mag.*, vol. 40, no. 3, pp. 35–48, Jun. 1998.

[2] R. K. Mongia and P. Bhartia, "Dielectric resonator antennas—A review and general design relations for resonant frequency and bandwidth," *Int. J. Microw. Millim. Wave Comput. Aided Eng.*, vol. 4, no. 3, pp. 230–247, 1994.

[3] K. S. Ryu and A. A. Kishk, "Ultrawideband dielectric resonator antenna with broadside patterns mounted on a vertical ground plane edge," *IEEE Trans. Antennas Propag.*, vol. 58, no. 4, pp. 1047–1053, Apr. 2010.

[4] C. A. Balanis, *Antenna Theory: Analysis and Design*, 3rd ed. Hoboken, NJ, USA: Wiley, 2005.

[5] Q. Rao, T. A. Denidni, and A. R. Sebak, "A new dual-frequency hybrid resonator antenna," *IEEE Trans. Antennas Propag. Lett.*, vol. 4, pp. 308–311, 2005.

[6] J.-Y. Kim, N. Kim, S. Lee, and B.-C. Oh, "Triple band-notched UWB monopole antenna with two resonator structures," *Microw. Opt. Technol. Lett.*, vol. 55, no. 1, pp. 4–6, 2013.

[7] Y. Ding and K. W. Leung, "On the dual-band DRA-slot hybrid antenna," *IEEE Trans. Antennas Propag.*, vol. 57, no. 3, pp. 624–630, Mar. 2009.

[8] Y.-F. Lin, H.-M. Chen, and C.-H. Lin, "Compact dual-band hybrid dielectric resonator antenna with radiating slot," *IEEE Antennas Wireless Propag. Lett.*, vol. 8, pp. 6–9, 2009.

[9] H.-M. Chen, Y.-K. Wang, Y.-F. Lin, S.-C. Lin, and S.-C. Pan, "A compact dual-band dielectric resonator antenna using a parasitic slot," *IEEE Antennas Wireless Propag. Lett.*, vol. 8, pp. 173–176, 2009.

[10] A. Sharma, P. Ranjan, and R. K. Gangwar, "Multiband cylindrical dielectric resonator antenna for WLAN/WiMAX application," *IET Electron. Lett.*, vol. 53, no. 3, pp. 132–134, 2017.

[11] Y. M. Pan, S. Y. Zheng, and W. Li, "Dual-band and dual-sense omnidirectional circularly polarized antenna," *IEEE Antennas Wireless Propag. Lett.*, vol. 13, pp. 706–709, 2014.

[12] H. S. Ngan, X. S. Fang, and K. W. Leung, "Design of dual-band circularly polarized dielectric resonator antenna using a higher-order mode," in *Proc. IEEE-APS APWC*, Sep. 2012, pp. 424–427.

[13] X. S. Fang, K. W. Leung, and E. H. Lim, "Singly-fed dual-band circularly polarized dielectric resonator antenna," *IEEE Antennas Wireless Propag. Lett.*, vol. 13, pp. 995–998, 2014.

[14] X. S. Fang and K. W. Leung, "Linear-/circular-polarization designs of dual-/wide-band cylindrical dielectric resonator antennas," *IEEE Trans. Antennas Propag.*, vol. 60, no. 6, pp. 2662–2671, Jun. 2012.

[15] M. Zhang, B. Li, and X. Lv, "Cross-slot-coupled wide dual-band circularly polarized rectangular dielectric resonator antenna," *IEEE Antennas Wireless Propag. Lett.*, vol. 13, pp. 532–535, 2014.

[16] A. Rashidian, L. Shafai, and D. M. Klymyshyn, "Compact wideband multimode dielectric resonator antennas fed with parallel standing strips," *IEEE Trans. Antennas Propag.*, vol. 60, no. 11, pp. 5021–5031, Nov. 2012.

[17] R. K. Mongia and A. Ittipiboon, "Theoretical and experimental investigations on rectangular dielectric resonator antennas," *IEEE Trans. Antennas Propag.*, vol. 45, no. 9, pp. 1348–1356, Sep. 1997.

[18] S. Fakhte, H. Oraizi, R. Karimian, and R. Fakhte, "A new wideband circularly polarized stair-shaped dielectric resonator antenna," *IEEE Trans. Antennas Propag.*, vol. 63, no. 4, pp. 1828–1832, Apr. 2015.

[19] G. Varshney, V. S. Pandey, R. S. Yaduvanshi, and L. Kumar, "Wide band circularly polarized dielectric resonator antenna with stair-shaped slot excitation," *IEEE Trans. Antennas Propag.*, vol. 65, no. 3, pp. 1380–1383, Mar. 2017.

[20] B. Li and K. W. Leung, "Strip-fed rectangular dielectric resonator antennas with/without a parasitic patch," *IEEE Trans. Antennas Propag.*, vol. 53, no. 7, pp. 2200–2207, Jul. 2005.

[21] W. L. Stutzman and G. A. Thiele, *Antenna Theory and Design*. Hoboken, NJ, USA: Wiley, 2013.

[22] B. Y. Toh, R. Cahill, and V. F. Fusco, "Understanding and measuring circular polarization," *IEEE Trans. Edu.*, vol. 46, no. 3, pp. 313–318, Aug. 2003.

ANSHUL GUPTA was born in Raipur, India, in 1987. He received the M.Tech. degree in microwave engineering from IIT (Banaras Hindu University) Varanasi, India, in 2011. He is currently pursuing the Ph.D. degree from the Electronics Engineering Department, IIT (Indian School of Mines), Dhanbad, India.

He joined the Department of Electronics and Telecommunication Engineering, National Institute of Technology at Raipur, Chhattisgarh, India, as an Assistant professor in 2013. He has authored or co-authored several research papers in international journals/conference proceedings. His current research interest includes dielectric resonator antennas, microstrip antennas, and FDTD techniques.

RAVI KUMAR GANGWAR (M'12) received the B.Tech. degree in electronics and communication engineering from Dr. A.P.J. Abdul Kalam Technical University, and the Ph.D. degree in electronics engineering from the IIT (Banaras Hindu University), Varanasi, India, in 2006 and 2011, respectively.

He is currently an Assistant Professor with the Department of Electronics Engineering, IIT (Indian School of Mines), Dhanbad, India. He has authored or co-authored over 100 research papers in international journals/conference proceedings. His research interest includes dielectric resonator antenna, microstrip antenna, and bio-electromagnetics.

He is a member of the Antenna and Propagation Society and the Communication Society, Institute of Electrical and Electronics Engineers (IEEE), USA. He is a Reviewer of the IEEE ANTENNA AND PROPAGATION LETTERS, *IET Microwaves and Antennas and Propagation*, the IEEE ELECTRONICS LETTERS, *Progress in Electromagnetic Research*, the *International Journal of RF, Microwave and Computer Aided Engineering*, the *International Journal of Electronics*, *International Journal of Microwave and Wireless Technology*, *Wireless Personal Communication*, the *Indian Journal of Radio and Space Physics*, and the *Indian Journal of Pure and Applied Physics*.